

Quantitative Observation of Backbone Disorder in Native Elastin*

Received for publication, October 3, 2003, and in revised form, November 17, 2003
Published, JBC Papers in Press, November 18, 2003, DOI 10.1074/jbc.M310948200

Maxim S. Pometun, Eduard Y. Chekmenev‡, and Richard J. Wittebort§

From the Department of Chemistry, University of Louisville, Louisville, Kentucky 40208

Elastin is a key protein in soft tissue function and pathology. Establishing a structural basis for understanding its reversible elasticity has proven to be difficult. Complementary to structure is the important aspect of flexibility and disorder in elastin. We have used solid-state NMR methods to examine polypeptide and hydrate ordering in both elastic (hydrated) and brittle (dry) elastin fibers and conclude (i) that tightly bound waters are absent in both dry and hydrated elastin and (ii) that the backbone in the hydrated protein is highly disordered with large amplitude motions. The hydrate was studied by ^2H and ^{17}O NMR, and the polypeptide by ^{13}C and ^2H NMR. Using a two-dimensional ^{13}C MAS method, an upper limit of $S < 0.1$ was determined for the backbone carbonyl group order parameter in hydrated elastin. For comparison, $S \sim 0.9$ in most proteins. The former result is substantiated by two additional observations: the absence of the characteristic ^2H spectrum for stationary amides and “solution-like” ^{13}C magic angle spinning spectra at 75°C , at which the material retains elasticity. Comparison of the observed shifts with accepted values for α -helices, β -sheets, or random coils indicates a random coil structure at all carbons. These conclusions are discussed in the context of known thermodynamic properties of elastin and, more generally, protein folding. Because coacervation is an entropy-driven process, it is enhanced by the observed backbone disorder, which, we suggest, is the result of high proline content. This view is supported by recent studies of recombinant elastin polypeptides with systematic proline substitutions.

Elastin, nature's elastomer, is a primary component in determining the mechanical properties of soft tissues. For example, deletion of the elastin gene is responsible for severe pathologies associated with Williams syndrome, and point mutations of the elastin gene are associated with obstructive vascular disease (1, 2). Recently, a variety of uses for elastin-like polypeptides containing a major elastin repeat (VPGVG) have been described. They include fusion proteins for rapid protein purification (3), artificial vascular tissues (4), biomolecular machines (5), and thermally targeted drugs (6). In these examples, a key property is an inverse transition that, like the coacervation of tropoelastin, occurs between 20 and 30°C .

A molecular basis for understanding elastin has been elusive, and difficulties arise from its inherent properties. It is, to

some degree, disordered, active only when swollen in water, insoluble, opaque and lacks long-range order. Thus, studies using solution NMR and optical spectroscopy are difficult and typically applied to either model compounds or non-native material. For example, circular dichroism of soluble (VPGVG) $_n$ and solid-state NMR of ((VPGVG) $_4$ (VPGKG)) $_{39}$ indicate the presence of β -turns (7, 8). A model for elastin based on β -turns, a β -spiral, has been proposed (9), and supporting evidence was reviewed recently (10). Structures containing β -sheets have also been proposed. ^{13}C NMR chemical shifts of lyophilized α -elastin (oxalic acid-extracted material), Fourier transform infrared spectroscopy of KBr pellets, and circular dichroism of KOH-solubilized elastin all indicate that sheets are a major structural element present in such material (11, 12). Finally, solid-state NMR studies of poly(LGGVG) indicate conformational heterogeneity (13).

Elastin's essential functional property, the ability to contract reversibly after stretching, is driven, at least in part, by an increase in entropy (10, 14, 15) and is closely related to disorder in the structure and its solvate. It is thus an example of a protein for which the interplay between structure and dynamics is crucial to function (16, 17). Long ago, Hoeve and Flory (14) proposed that elastin is analogous to natural rubbers, *i.e.* polypeptide chains are completely disordered with a gaussian distribution of end-to-end distances. Backbone motions were confirmed by dielectric (18) and NMR (19–21) relaxation studies that focused on the time scale of the dynamics. In addition, from the absence of intrinsic birefringence, it was concluded that elastin is isotropic and devoid of structure at the molecular level (22, 23). A qualitatively different mechanism based on librational entropy of a β -spiral structure was proposed by Urry (24). Support for this picture includes the observation of a slow, thermally induced decrease in thermoelasticity that was attributed to unfolding of the β -spiral (24). This model is not, however, supported by recent molecular dynamics (MD)¹ simulations of hydrated (VPGVG) $_{18}$ (25–27). Starting with a β -spiral structure, a high degree of disorder inconsistent with a well defined 2° structure develops on a time scale of ~ 10 ns. The experimentally observed inverse transition is predicted and shown to be a hydrophobic collapse to a dynamic globular structure containing distorted β -turns and β -sheets. Testable predictions of these calculations include a backbone order parameter with a value of $S \sim 0.51$ (25), which is small, for example, compared with $S = 0.9$ determined by solid-state NMR for the well ordered backbone amides in crystalline lysozyme (28).

A key aspect of this study is the determination of polypeptide and hydrate order parameters in both elastic (hydrated) and brittle (dry) elastin based on measurements of residual anisotropic couplings by solid-state ^{13}C , ^2H , and ^{17}O NMR. From ^{17}O and ^2H NMR, we conclude that tightly bound waters are absent

* The costs of publication of this article were defrayed in part by the payment of page charges. This article must therefore be hereby marked “advertisement” in accordance with 18 U.S.C. Section 1734 solely to indicate this fact.

‡ Present address: National High Magnetic Field Lab., Florida State University, Tallahassee, FL 32310.

§ To whom correspondence should be addressed: Dept. of Chemistry, University of Louisville, 2320 S. Brook St., Louisville, KY 40208. Tel.: 502-852-6613; Fax: 502-852-8149; E-mail, rjwitt01@louisville.edu.

¹ The abbreviations used are: MD, molecular dynamics; MAS, magic angle spinning; T, tesla(s).

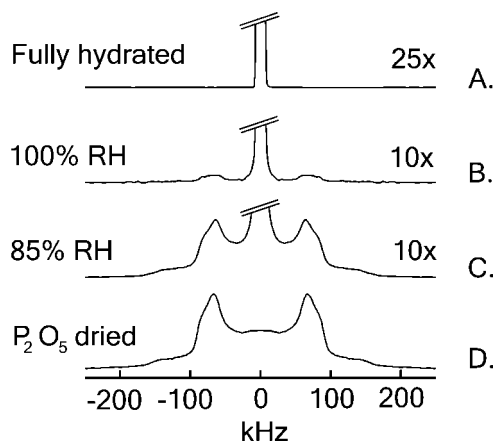


FIG. 1. 11.7-T ^2H NMR spectra of elastin fibers fully hydrated (A), equilibrated to a relative humidity of 100% (B) or 85% (C), and dried over P_2O_5 (D). RH, relative humidity.

and that the elastin hydrate reorients isotropically. Similarly, the absence of any solid-like ^2H signal, which is readily observed for stationary amides in dry elastin, suggests the possibility of large amplitude motions in the backbone of the hydrated protein. This disorder was directly observed using a two-dimensional ^{13}C magic angle spinning (MAS) method that separates anisotropic and isotropic chemical shielding. In contrast to dry material, near-zero anisotropic chemical shielding at all carbon sites was observed for hydrated material, substantiating that the protein is highly disordered on a time scale of 50 μs . ^{13}C spectra of stretched fibers show an increase in chain ordering and/or a slowing of molecular dynamics. Finally, we found that well resolved “solution-like” ^{13}C MAS spectra were obtained at high field (18.8 T) and 75 $^\circ\text{C}$. At this temperature, the material retains its characteristic elasticity, and comparison of the observed shifts with reference values for α -helices, β -sheets, or random coils (29) indicates a random coil structure.

EXPERIMENTAL PROCEDURES

Elastin fibers from bovine neck ligament, prepared by the neutral extraction method (30), were purchased from Elastin Products Co., Inc. (Owensville, MO). $^2\text{H}_2\text{O}$ and H_2^{17}O were obtained from ISOTECH (Miamisburg, OH).

Stationary ^{13}C , ^2H , and ^{17}O spectra were recorded on a lab-built 11.7-T (500 MHz for ^1H) spectrometer with double-resonance probes. The ^{13}C 2D-PASS experiment (31) was implemented with 16 increments in t_1 on the same instrument using a lab-built 4-mm MAS probe. To obtain more easily interpretable two-dimensional contour plots, data tables were sheared and interpolated in f_1 (31). Variable temperature ^{13}C MAS spectra were recorded on a Varian Inova 800 instrument with a 3.2-mm triple-resonance MAS probe. Dehydration of the sample while in the MAS rotor was eliminated by the use of tightly fitting caps. Cross-polarization spectra of dry fibers were obtained with contact times from 1.2 to 1.6 ms and matched Hartman-Hahn field strengths of 50–80 kHz. Direct polarization spectra of hydrated fibers were obtained with ^{13}C pulse widths of 5 μs (11.7 T) or 3.5 μs (18.8 T). The ^1H decoupling field strengths were 100 kHz (11.7 T) or 60 kHz (18.8 T). ^{13}C MAS spectra were externally referenced to DSS (32) and processed using the manufacturer’s software (Varian). A resolution enhancement protocol was used that decreased line widths by $\sim 25\%$ and that introduced little phase distortion (gaussian broadening with $gf = 0.012$ s, sine bell with $sb = 0.012$ s, and the sine bell offset with $sbs = 0.0056$ s). Transverse relaxation rates ($1/T_2$) were determined with a Hahn spin echo (33) and compared with line widths from spectra processed without digital filtering.

The upper limit for the backbone order parameters was determined by simulating the side band intensities for the ^{13}C MAS spectrum at the spinning frequency (3.6 kHz) with the approximation that the residual shielding tensor is axially symmetric, a reasonable assumption because the residual anisotropy is quite small. The residual anisotropy (tensor span), $\Delta\sigma$, was systematically decreased to the point at which the ratio of the center band to the larger of the ± 1 side bands equaled the

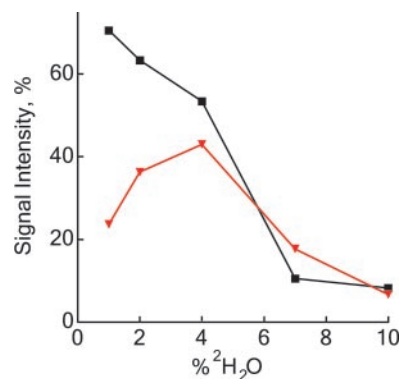


FIG. 2. ^2H solid signal intensity of elastin fibers equilibrated in a $^2\text{H}_2\text{O}$ /acetone mixed solvent. The sample initially exchanged in $^2\text{H}_2\text{O}$ (black squares) exhibited a decrease in the solid ^2H signal upon rehydration in the mixed solvent, whereas the sample initially exchanged in H_2O (red inverted triangles) first showed an increase and subsequently decreased with higher water activity. Signal intensities are expressed relative to an elastin sample exchanged in $^2\text{H}_2\text{O}$ and dried under vacuum (100% intensity).

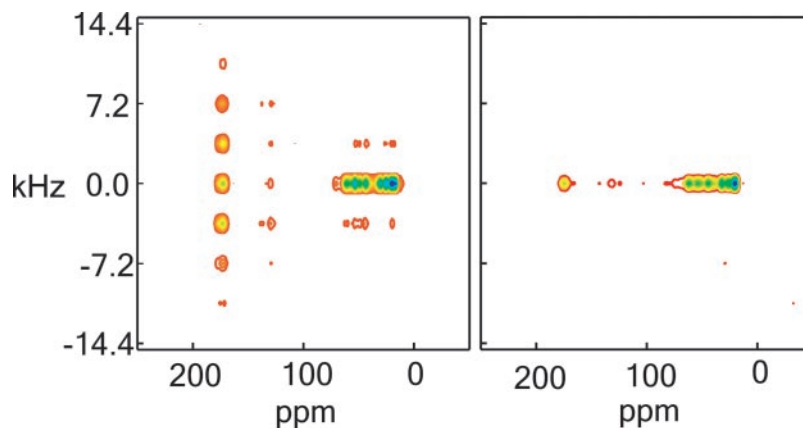
signal-to-noise ratio (57:1) observed in the experimental spectrum for the carbonyl carbons. Finally, using the anisotropy of $\Delta\sigma = (\sigma_{11} - \sigma_{33})$ ppm observed in dry elastin, which is in good accord with known static anisotropies for peptide carbonyls (34), the order parameter is calculated as $S = \Delta\sigma/\Delta\sigma$ (35).

RESULTS

^2H , ^{17}O , and ^{13}C Solid-state NMR and Dynamics—In the NMR experiments used here, the effect of dynamics on the observed spectrum depends on the rate or reciprocal correlation time ($1/\tau_c$) in comparison with the anisotropy of the spin coupling (ν_{aniso}). Approximately speaking, ν_{aniso} is the breadth of the NMR spectrum observed in a randomly oriented sample in the static or slow exchange limit, $1/\tau_c \ll \nu_{\text{aniso}}$ (36). For the ^2H and ^{17}O experiments, $\nu_{\text{aniso}} \sim 200$ and 50 kHz and arises from first- and second-order quadrupole interactions, respectively. For ^{13}C at a magnetic field of 11.7 T, the relevant interaction is chemical shielding with $\nu_{\text{aniso}} \sim 20$ kHz for C' or $\nu_{\text{aniso}} \sim 5$ kHz for aliphatics such as C^α . Importantly, when the dynamical rate is fast compared with the anisotropy ($1/\tau_c \gg \nu_{\text{aniso}}$), analysis of the solid-state NMR spectrum depends only on the distribution of orientations, *i.e.* the motional amplitudes. Consequently, fast motions average the anisotropic coupling to some residual or averaged value ($\bar{\nu}_{\text{aniso}}$) determined by the distribution of orientations sampled. In the special case where both the static coupling and dynamical process have axial symmetry, the usual order parameter is readily calculated as $S = \bar{\nu}_{\text{aniso}}/\nu_{\text{aniso}}$ (35). For example, when fast motions are isotropic ($S = 0$), narrow spectroscopic lines are observed ($\bar{\nu}_{\text{aniso}} = 0$). In a randomly oriented solid, spectral patterns rather than narrow lines are typically observed as a consequence of spatially anisotropic spin interactions. Because ν_{aniso} varies from 5 to 200 kHz in the NMR experiments used here, we have some flexibility to choose an experiment to avoid the more complicated intermediate exchange regime ($1/\tau_c \sim \nu_{\text{aniso}}$), in which spectra depend on both motional rates and amplitudes.

Bound Waters Are Absent, and Amides Are Dynamic— ^2H and ^{17}O NMR are complementary for examining ordering of both hydrate and amide groups (37). When the solid protein is exhaustively exchanged with isotopically enriched water, $^2\text{H}_2\text{O}$ labels both hydrate and exchangeable hydrogens (primarily amides), whereas H_2^{17}O labels exclusively the hydrate. In Fig. 1, ^2H NMR spectra of ^2H -labeled elastin fibers equilibrated to several hydration levels are shown. The spectrum from fully hydrated and elastic material ($\times 25$ vertical expansion) is dominated by a sharp signal indicative of isotropically reorienting

FIG. 3. 11.7-T 2D-PASS spectra of dry (left panel) and hydrated (right panel) elastin at a spinning speed of 3.6 kHz. Whereas dry elastin showed, for example, a C' signal with the characteristic span (~150 ppm) for a stationary backbone, the hydrated material exhibited a complete absence of spinning side bands, indicating near-zero anisotropies for all the carbons.



deuterons and shows no evidence of a solid-like ^2H signal (Fig. 1A). In contrast, after extensive drying over P_2O_5 , a prominent solid-like pattern with well defined quadrupole coupling ($\chi_{zz} = 200$ kHz) and asymmetry ($\eta = 0.13$) was obtained from inelastic fibers (Fig. 1D). Although the solid-like ^2H signal is potentially from bound hydrate and amide deuterons, the asymmetry is more nearly that of H-bonded amides ($\eta \sim 0.14$) (38) than H-bonded water ($\eta \sim 0.10$) (39), and assignment to amides was confirmed by ^{17}O NMR and thermal gravimetry. Whereas ^{17}O cross-polarization spectra of peptide hydrates show characteristic ^{17}O spectra ($\chi_{zz} \sim 6$ MHz and $\eta \sim 1$) (37), no solid-like or isotropic ^{17}O signal was observed in fibers swollen in H_2^{17}O and subsequently dried over P_2O_5 (data not shown). Moreover, weight loss determined by thermal gravimetry analysis was negligible (<1.5%) from 30 to 80 °C and not measurable from 80 to 130 °C. Together, these experiments demonstrate that elastin lacks strongly bound hydrate when fully hydrated or dried over P_2O_5 and that the characteristic “solid” ^2H signal from stationary amides, readily observed in dry elastin, is absent in fully elastic material.

By establishing more precise control over the level of hydration, we show a direct correlation between the loss of the ^2H amide signal and the onset of elasticity. The thermodynamic activity of water is varied either by equilibrating fibers against an atmosphere of known relative humidity (40) or by swelling fibers in a mixed solvent. Elasticity is judged qualitatively by the extensibility compared with fibers in excess water. When equilibrated to a relative humidity of 85%, marginally elastic material was obtained wherein fibers could be stretched to ~120% of their relaxed length and did not readily retract (Fig. 1C). The spectrum shows an ~10-fold reduction in intensity compared with the solid-like spectrum of dry material (Fig. 1D). Increasing the relative humidity to 100% gave elasticity approaching the fully hydrated state (reversibly extensible to ~150% of the relaxed length) and largely eliminated the solid-like ^2H spectrum (Fig. 1C).

Better control of the thermodynamic activity of water is obtained with a mixed solvent system, and we found that elastin fibers were fully extensible in water/acetone solutions containing a small percentage of water (>8%). In these experiments, fibers were exhaustively exchanged against either H_2O or $^2\text{H}_2\text{O}$, dried under vacuum, and then equilibrated in acetone/ $^2\text{H}_2\text{O}$ (overnight) for ^2H spectroscopy. In Fig. 2, the intensity of the solid-like ^2H signal is correlated with the percent $^2\text{H}_2\text{O}$ in the mixed solvent. Fibers initially exchanged against $^2\text{H}_2\text{O}$ and equilibrated in solvent with less than ~5% $^2\text{H}_2\text{O}$ were not elastic and yielded substantial solid ^2H signals, whereas the spectra of fully elastic fibers (greater than ~8% $^2\text{H}_2\text{O}$) are comparable with those of fibers at 100% relative humidity or in excess water and have no solid signal. Moreover, the signal

decreased monotonically with increasing percent $^2\text{H}_2\text{O}$. A different pattern was observed for elastin initially exchanged in unlabeled H_2O . Here, the solid ^2H signal initially increased and subsequently decreased, indicating that amide sites in dry fibers are not readily accessible, but that, with the onset of elasticity, amide exchange labeling occurs.

Thus, with the onset of elasticity, amide groups are not protected by strong $\text{N-H}\cdots\text{O}=\text{C}$ hydrogen bonding; and in fully elastic material (in excess water at 100% relative humidity and in the mixed solvent with >8% water), the absence of the solid ^2H signal indicates that the backbone is dynamic. If the reorientational rate is comparable with the quadrupole coupling ($1/\tau_c \sim 200$ kHz), then the ^2H signal would be difficult to observe (36, 37), and no quantitative conclusion can be drawn about the amplitude of the motion. Alternatively, if the motion is fast, then the ^2H amide signal overlaps with the sharp solvent signal, indicating that backbone reorientation is essentially isotropic. This ambiguity is resolved by ^{13}C experiments described below.

^{13}C Shielding Anisotropy in Hydrated Elastin Is Negligible, Indicating Large Amplitude Motions—A high degree of conformational flexibility in the polypeptide backbone is quantitatively assessed based on the degree of motional averaging of ^{13}C shielding anisotropies. In this experiment, the spectrum arises only from non-labile sites on the protein, and a two-dimensional approach, 2D-PASS (31), that places isotropic shifts and shielding anisotropy on orthogonal axes was used. In Fig. 3, different carbon types are separated along the horizontal axis by their characteristic isotropic chemical shifts, whereas the number and intensities of spinning side bands along the vertical axis are directly related to the shielding anisotropy. Because the side bands are spaced at the spinning frequency, a slow spinning speed of 3.6 kHz was used, which is sufficient to observe shielding anisotropies of 10 ppm or larger. The spectrum from dry elastin was obtained with cross-polarization, whereas direct polarization is required to obtain adequate signal from fully swollen material (41). Dry fibers exhibited relatively broad lines and isotropic shifts for the major carbon types: carbonyls (~170 ppm), aromatic side chains (131 ppm), and aliphatic carbons (10–70 ppm). In dry material, a shielding span ($\sigma_{11} - \sigma_{33}$) of 150 ppm was deduced from the C' side band pattern using standard analysis (31). This is the expected value for a typical stationary peptide carbonyl (34), and a similar anisotropy is seen for the aromatic carbons. Also, the expected and smaller static anisotropies (30–50 ppm) are indicated for aliphatic carbons that show fewer side bands. A striking result is seen in the spectra of hydrated material at 20 °C (Fig. 3) and 37 °C (data not shown). At both temperatures, there was a complete absence of spinning side bands, indicating very small residual anisotropies at all carbons and

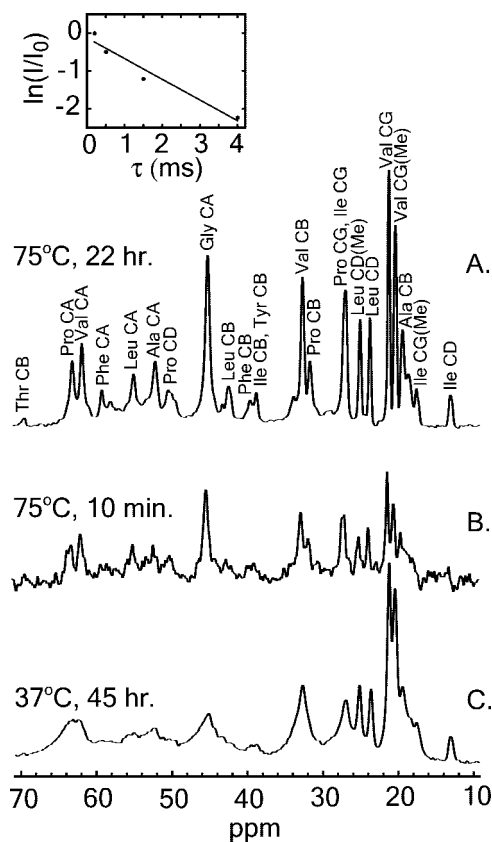


FIG. 4. 18.8-T ^{13}C MAS NMR spectra of hydrated elastin at a spinning speed of 8 kHz and at 75 °C (A and B) or 37 °C (C). Equivalent spectral features and chemical shifts are seen in both the high signal-to-noise spectrum (A) and when the spectrum was obtained quickly (B) such that the sample was only briefly raised to 75 °C. At 37 °C, resolution was poorer due primarily to increased line widths (C). The Ile C^β signal is well resolved, and the chemical shift (13.2 ppm) does not change from 37 to 75 °C. Results of the T_2 measurement are shown in the inset for the Gly C^α signal at 45.40 ppm ($1/\pi T_2 = 155 \pm 30$ Hz). CB, C^β ; CA, C^α ; CD, C^δ ; CG, C^γ .

thus confirming the presence of large amplitude motions in the protein backbone. Based on the signal-to-noise ratio (57:1) of the C' center band and the absence of observable side bands, we estimate an upper limit to the C' residual shielding in hydrated elastin at 37 °C of 14 ppm, corresponding to a backbone carbonyl order parameter of $S < 0.1$ (see "Experimental Procedures"). We note that a model elastin polypeptide, $((\text{VPGVG})_4(\text{VPGKG}))_{39}$, shows static shielding anisotropies. However, as hydration was increased, cross-polarization NMR signals were reported to decrease due to molecular motions (8). Insofar as direct polarization rather than cross-polarization is required to obtain good spectra of fully hydrated elastin, comparison of the two systems would require spectra of fully swollen (cross-linked) proteins in both cases.

^{13}C Shifts Are Comparable with Random Coil Values—With increasing temperature, resolution of the ^{13}C MAS spectrum of hydrated elastin increased substantially, and a well resolved spectrum was reproducibly obtained in an 18.8-T instrument at 75 °C (Fig. 4). Although many proteins are denatured at this temperature, samples studied at 75 °C showed reversible elasticity before and after the NMR experiments, which was expected based on previous observations. Thermoelastic studies show that the force generated by elastin fibers increases somewhat between 60 and 75 °C (9), and the irreversible decrease in the thermoelasticity of elastin at 80 °C occurs with a half-life of 10 days (24). The spectrum in Fig. 4A was accumulated in a comparatively short time (22 h), and a spectrum accumulated

in even less time (10 min) had a sufficient signal-to-noise ratio to confirm the observed spectral features (Fig. 4B). At 37 °C, many of the spectral features seen at 75 °C were still evident, but resolution had decreased due to increased line widths (Fig. 4C). The origin of increased line widths ($\Delta\nu$) at lower temperature is due either to an increased range of isotropic shifts corresponding to different conformations or to efficient transverse relaxation. The contribution of the latter ($1/\pi T_2$) to the observed line widths can be measured directly with a Hahn spin echo experiment at 75 °C (33). The result for a representative peak (the resolved line at 45.4 ppm assigned to Gly C^α) is shown in Fig. 4 (inset). At 75 °C, the transverse relaxation contribution to the line width ($1/\pi T_2 = 155 \pm 30$ Hz) accounts for the observed line width ($\Delta\nu \approx 140$ Hz), indicating that chemical shift dispersion within a given line is comparatively small. Note that the transverse relaxation rate ($1/T_2 \sim 500$ s $^{-1}$) is fast compared with the longitudinal rate ($1/T_1 > 1$ s $^{-1}$) and thus indicates the presence of slow motions in elastin ($1/\tau_c < 10^9$ s $^{-1}$).

The excellent resolution of the MAS spectra (0.7 ppm line widths) provides chemical shifts, which are reliable probes for distinguishing among α -helix, β -sheet, and random coil structures (29). The spectral assignments in Fig. 4 are based on the chemical shift index (29) and the known composition of bovine elastin (NCBI accession number NP_786966). For example, the intensities of all resolved C^α signals are in excellent agreement with their respective abundance, except for alanine. The low alanine intensity is expected because most occur in cross-linking regions that have previously been shown to be more motionally restricted than hydrophobic domains (19). In proteins, C^α helix values are ~ 4 ppm downfield of sheet values, whereas C^β helix values are upfield by ~ 3 ppm, and random coil shifts are intermediate as a consequence of averaging over accessible conformations. As shown in Table I, the five most abundant amino acids in elastin ($\sim 84\%$ of the total sequence) all have C^α isotropic chemical shifts within 0.5 ppm of random coil values, with an average deviation of 0.1 ppm. In contrast, data base values for helices and sheets are, on average, 2.5 ppm downfield and 0.8 ppm upfield, respectively, of the observed values. Similarly, for C^β , the average deviation from random coil chemical shifts is 0.2 ppm, and the reference values are either upfield (α -helix) or downfield (β -sheet) by 1 ppm on average. Furthermore, isotropic shifts for the other side chain carbons are very close to known average chemical shifts. A noteworthy example is the Ile C^β signal at 13.2 ppm, which appears as a single, well resolved signal at 37 and 75 °C (Fig. 4). Chemical shifts for this site in proteins vary over an unusually large range (from 3.2 to 21.3 ppm), and the observed shift is within 0.14 ppm of the average observed in all proteins (29). To summarize the chemical shift data, we note that S.D. values of the 2° structure shifts (~ 1.8 ppm for C^α) (29) indicate that we cannot completely exclude β -sheets or β -turns, which are not well characterized. Overall, however, the observed shifts are best described as random coil and without exception.

Stretching Slows Dynamics or Increases Order— ^{13}C NMR spectra of a single hydrated elastin fiber in relaxed and stretched states were obtained using the sample arrangement shown in Fig. 5. Stationary spectra of relaxed fibers are essentially equivalent to the MAS spectra, but with lower resolution. Nevertheless, the C' signal, which exhibited the largest anisotropy in dry elastin, is well resolved from the aliphatic carbons. Compared with the spectrum of relaxed material, that obtained when the fiber was stretched to 150% of the relaxed length shows somewhat broader signals, most notably from the peptide carbonyl groups. This is due to increased shielding anisotropy, *i.e.* increased ordering in the backbone, and/or to more

TABLE I
Observed C^α and C^β chemical shifts for major residues in hydrated elastin and comparison with known values (29) for different secondary structures

ΔCoil , $\Delta\alpha$, and $\Delta\beta$ are the differences between the data base chemical shifts for the random coil, α -helix, and β -sheet, respectively, and the observed chemical shifts. All shifts are referenced to DSS.

Residue	Abundance	Observed	ΔCoil	$\Delta\alpha$	$\Delta\beta$
	%				
Ala C^α	~21	52.35	0.49	2.48	-0.82
Gly C^α	~31	45.40	0.11	1.51	-0.18
Leu C^α	~11	55.20	-0.28	2.32	-1.12
Pro C^α	~12	63.35	0.12	2.14	-0.71
Val C^α	~1	62.08	-0.02	4.08	-1.25
Ala C^β	~21	19.56	-0.50	-1.30	1.58
Ile C^β	~3	38.95	-0.30	-1.35	0.91
Leu C^β	~11	42.62	-0.24	-0.97	1.17
Pro C^β	~12	31.83	0.11	-0.37	0.44
Val C^β	~13	32.80	-0.09	-1.31	1.11

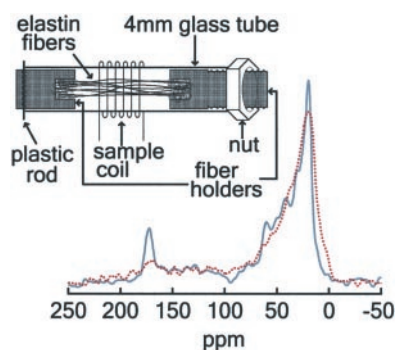


FIG. 5. ^{13}C NMR spectra (direct polarization) of hydrated elastin in relaxed and stretched states and the apparatus for stretching the fibers. Relaxed elastin (solid line) yielded a spectrum very similar to that of randomly oriented fibers, *i.e.* negligible anisotropy was observed. Stretched fibers (dotted line) showed broadening of the carbonyl and methyl ^{13}C signals, indicating increased ordering and/or slowed dynamics upon stretching.

efficient transverse relaxation from a slowing of molecular motions. The former would imply a decrease in chain entropy upon stretching (42, 43), whereas the latter is consistent with thermodynamic (15) and MD (44) simulations, suggesting that the entropic driving force for elasticity is associated with the solvent rather than with the polypeptide chain.

DISCUSSION

A variety of solid-state NMR experiments with native elastin are presented here. The primary focus of these experiments was to determine the degree of spatial averaging in hydrated elastin, and all results indicate that functional elastin is highly disordered. From the two-dimensional ^{13}C MAS experiment, we determined an upper limit to the backbone order parameter of $S < 0.1$ at 37 °C. Moreover, a similarly high degree of disorder was observed at all temperatures examined from 20 to 75 °C. A useful, albeit approximate model frequently used for interpreting backbone order parameters is based on the picture of a vector rotationally diffusing within a cone of semiangle θ_0 . In this model, $S = \cos\theta_0(1 + \cos\theta_0)/2$ (45), and the upper limit for S established here corresponds to $\theta_0 > 80^\circ$. This is pictorially represented for a peptide fragment in Fig. 6, in which the orientation of each carbonyl $\text{C}=\text{O}$ bond explores a near hemispherical space as a result of motion in the torsion angles. A particular torsion (those in a Pro-Gly fragment, for example) (8, 13) could have a preferred value. However, for all carbonyl bonds to reorient when viewed by a stationary observer, neighboring torsions must sample a large space. Models that favor a small region of conformational space are inconsistent with these observations.

This result is directly supported by the ^2H experiments

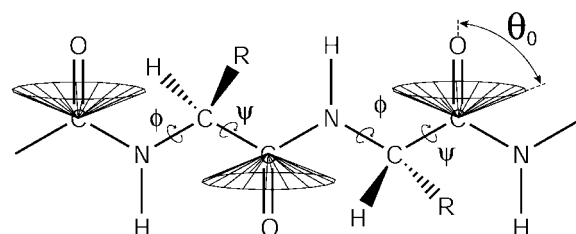


FIG. 6. Pictorial representation of disorder for carbonyl groups with order parameters of 0.1. The cones represent the conformational space (cone with semiangle of 80°) explored by $\text{C}=\text{O}$ orientations on a time scale of 50 μs .

showing that the characteristic ^2H spectrum for stationary amides systematically disappears upon hydration and that the amide groups are exchange-labile and not strongly H-bonded. Also, the ^2H and ^{17}O experiments indicate an absence of strongly bound waters. Ordered clathrate water is an important aspect of the entropy-driven contraction of elastin (15) and the coacervation of tropoelastin (46). That such water is not observed here indicates that it is in rapid exchange with bulk water. This feature is distinct from the collagen structure, for example, in which tightly bound waters have been directly observed using the solid-state NMR methods used here.²

Similarly, chemical shifts from 18.8-T ^{13}C MAS spectra are in excellent agreement with accepted values for a random coil (29). Although the ^{13}C chemical shifts were obtained at a temperature that is above the physiological range, the NMR samples showed reversible elasticity, and the spectra were obtained in a short time compared with that previously found for the irreversible loss of elasticity at 80 °C (24).

The observations reported here are in agreement with previous NMR and optical birefringence studies on native material (19–22). They are also consistent with recent MD simulations of an elastin-like polypeptide, (VPGVG)₁₈. The discrepancy with the somewhat larger MD backbone amide order parameters ($S = 0.51$) (25) is likely due to the much shorter time scale (~ 10 ns) of the MD calculations compared with that of the NMR experiment (~ 50 μs). In this regard, the presence of slow molecular motions ($1/\tau_c < 10^9$ s⁻¹) was confirmed. The MD calculations are inconsistent with a β -spiral-type structure for elastin (25–27, 44) and the even smaller NMR order parameter observed here is strong experimental evidence against this or any model with stable 2° structure.

Elastin's high degree of dynamic disorder distinguishes it from most native proteins; and to summarize our findings, we have considered this in the context of protein folding. Two

² A. M. Clark, K. V. Lakshmi, D. K. Lee, and R. J. Wittebort, manuscript in preparation.

important processes in protein folding are a hydrophobic collapse (48) and the formation of rudimentary 2° structures (49, 50). The occurrence of the former in (VPGVG)_n (10) or tropoelastin (51) is clearly displayed by the inverse transitions and has the signature of an entropy-driven process ($\Delta S > 0$). For example, decreasing the hydrophobicity of (VPGVG)_n with Val-to-Glu substitutions increases the inverse transition temperature by 24 °C (52). Force generation in mature cross-linked elastin has been correlated with this hydrophobic collapse (25–27), and the characteristic large negative enthalpy (53) upon stretching elastin indicates that the concomitant exposure of hydrophobic side chains is the mechanism of elasticity (15). Regarding the formation of 2° structure, the NMR evidence presented here shows that backbone ordering is largely absent over a temperature range including 37 °C. In contrast to the hydrophobic collapse, formation of 2° structure is an enthalpic process ($\Delta S < 0$) and compensates the entropy change from the former. An interesting example is the formation of β -sheet-type folding intermediates in an Ig domain wherein entropy changes for collapse and 2° structure formation cancel, resulting in no temperature dependence in the folding intermediate population (54). Thus, the presence of the inverse transition, in particular at lower temperatures, is consistent with a highly disordered polypeptide and suggests that an important feature of elastin is a sequence with a low propensity for any 2° structure. Chou-Fasman propensities, for example, indicate that the high frequencies of proline and glycine in elastin should inhibit both sheet and helix formation. The elastic domain in muscle fiber titin is also rich in proline, and it is proposed to lack 2° structure (47). Recently, Keeley and co-workers (46) reported coacervation temperatures for systematic mutation of proline residues in recombinant proteins containing both elastin hydrophobic and linker domains. It was found, somewhat surprisingly, that increasing backbone flexibility by decreasing the proline content (replacing the pentapeptide repeat PGVGV with the hexapeptide PGVGVVA) raised the coacervation temperature. This observation is, however, consistent with proline increasing backbone disorder. Furthermore, mutation of all proline residues to glycine eliminated coacervation and yielded a structure of amyloid-type β -sheets. Keeley and co-workers pointed out that the presence of proline is an important factor in preventing the formation of structures that allow amyloid-type aggregation. Based on the observations presented here showing that the backbone is highly disordered in elastic material, we suggest that high proline content prevents other 2° structures as well.

Note Added in Proof—In a recent article by Perry *et al.* (Perry, A., Stypa, M. P., Foster, J. A., and Kumashiro, K. K. (2002) *J. Am. Chem. Soc.* **124**, 6832–6833), ¹³C spectra of specifically labeled, hydrated elastin obtained from cell culture are reported. The gly C' line width in non-spinning spectra show negligible shielding anisotropy with a residual line width of ~6 ppm. This result is in complete agreement with the measurements presented here indicating a residual shielding anisotropy of less than 14 ppm for C' from Gly and other residue types.

REFERENCES

- Brooke, B. S., Bayes-Genis, A., and Li, D. Y. (2003) *Trends Cardiovasc. Med.* **13**, 176–181
- Li, D. Y., Toland, A. E., Boak, B. B., Atkinson, D. L., Ensing, G. J., Morris, C. A., and Keating, M. T. (1997) *Hum. Mol. Genet.* **6**, 1021–1028
- Meyer, D. E., and Chilkoti, A. (1999) *Nat. Biotechnol.* **17**, 1112–1115
- Welsh, E. R., and Tirrell, D. A. (2000) *Biomacromolecules* **1**, 23–30
- Urry, D. W. (1995) *Sci. Am.* **272**, 64–69
- Meyer, D. E., Shin, B. C., Kong, G. A., Dewhirst, M. W., and Chilkoti, A. (2001) *J. Controlled Release* **74**, 213–224
- Urry, D. W., Trapane, T. L., and Prasad, K. U. (1985) *Biopolymers* **24**, 2345–2356
- Hong, M., Isailovic, D., McMillan, R. A., and Conticello, V. P. (2003) *Biopolymers* **70**, 158–168
- Urry, D. W. (1988) *J. Protein Chem.* **7**, 1–34
- Urry, D. W., Hugel, T., Seitz, M., Gaub, H. E., Sheiba, L., Dea, J., Xu, J., and Parker, T. (2002) *Philos. Trans. R. Soc. Lond. Ser. B Biol. Sci.* **357**, 169–184
- Kumashiro, K. K., Kim, M. S., Kaczmarek, S. E., Sandberg, L. B., and Boyd, C. D. (2001) *Biopolymers* **59**, 266–275
- Debelle, L., Alix, A. J. P., Jacob, M. P., Huvenne, J. P., Berjot, M., Sombret, B., and Legrand, P. (1995) *J. Biol. Chem.* **270**, 26099–26103
- Kumashiro, K. K., Kurano, T. L., Niemczura, W. P., Martino, M., and Tamburro, A. M. (2003) *Biopolymers* **70**, 221–226
- Hoeve, C. A. J., and Flory, P. J. (1974) *Biopolymers* **13**, 677–686
- Gosline, J. M. (1978) *Biopolymers* **17**, 677–695
- Wand, A. J. (2001) *Nat. Struct. Biol.* **8**, 926–931
- Lee, A. L., and Wand, A. J. (2001) *Nature* **411**, 501–504
- Urry, D. W., Peng, S. Q., Xu, J., and McPherson, D. T. (1997) *J. Am. Chem. Soc.* **119**, 1161–1162
- Torchia, D. A., and Piez, K. A. (1973) *J. Mol. Biol.* **76**, 419–424
- Lyerla, J. R., and Torchia, D. A. (1975) *Biochemistry* **14**, 5175–5183
- Fleming, W. W., Sullivan, C. E., and Torchia, D. A. (1978) *Biophys. J.* **21**, A39
- Aaron, B. B., and Gosline, J. M. (1980) *Nature* **287**, 865–867
- Aaron, B. B., and Gosline, J. M. (1981) *Biopolymers* **20**, 1247–1260
- Urry, D. W. (1988) *J. Protein Chem.* **7**, 81–114
- Li, B., Alonso, D. O. V., and Daggett, V. (2001) *J. Mol. Biol.* **305**, 581–592
- Li, B., and Daggett, V. (2002) *J. Muscle Res. Cell Motil.* **23**, 561–573
- Li, B., and Daggett, V. (2003) *Biopolymers* **68**, 121–129
- Mack, J. W., Usha, M. G., Long, J., Griffin, R. G., and Wittebort, R. J. (2000) *Biopolymers* **53**, 9–18
- Zhang, H. Y., Neal, S., and Wishart, D. S. (2003) *J. Biomol. NMR* **25**, 173–195
- Partridge, S. M., Davis, H. F., and Adair, G. S. (1955) *Biochem. J.* **61**, 11–21
- Antzutkin, O. N., Shekar, S. C., and Levitt, M. H. (1995) *J. Magn. Reson. Ser. A* **115**, 7–19
- Wishart, D. S., Bigam, C. G., Yao, J., Abildgaard, F., Dyson, H. J., Oldfield, E., Markley, J. L., and Sykes, B. D. (1995) *J. Biomol. NMR* **6**, 135–140
- Hahn, E. L. (1950) *Phys. Rev.* **80**, 580–594
- Duncan, T. M. (1997) *Principal Components of Chemical Shift Tensors*, 2nd Ed., pp. 40–42, Farragut Press, Madison, WI
- Seelig, J., and Seelig, A. (1980) *Q. Rev. Biophys.* **13**, 19–61
- Wittebort, R. J., Olejniczak, E. T., and Griffin, R. G. (1987) *J. Chem. Phys.* **86**, 5411–5420
- Pometun, M. S., Gundusharma, U. M., Richardson, J. F., and Wittebort, R. J. (2002) *J. Am. Chem. Soc.* **124**, 2345–2351
- Usha, M. G., Peticolas, W. L., and Wittebort, R. J. (1991) *Biochemistry* **30**, 3955–3962
- Wittebort, R. J., Usha, M. G., Ruben, D. J., Wemmer, D. E., and Pines, A. (1988) *J. Am. Chem. Soc.* **110**, 5668–5671
- Preis, I. R., and Skhirtladze, G. I. (1976) *Zh. Fiz. Khimii* **50**, 736–737
- Perry, A., Stypa, M. P., Tenn, B. K., and Kumashiro, K. K. (2002) *Biophys. J.* **82**, 1086–1095
- Akke, M., Bruschweiler, R., and Palmer, A. G. (1993) *J. Am. Chem. Soc.* **115**, 9832–9833
- Li, Z. G., Raychaudhuri, S., and Wand, A. J. (1996) *Protein Sci.* **5**, 2647–2650
- Li, B., Alonso, D. O. V., Bennion, B. J., and Daggett, V. (2001) *J. Am. Chem. Soc.* **123**, 11991–11998
- Lipari, G., and Szabo, A. (1980) *Biophys. J.* **30**, 489–506
- Miao, M., Bellingham, C. M., Stahl, R., Sitarz, E., Lane, C., and Keeley, F. W. (2003) *J. Biol. Chem.* **278**, 48553–48562
- Reiersen, H., and Rees, A. R. (2001) *Trends Biochem. Sci.* **26**, 679–684
- Chan, H. S., and Dill, K. A. (1990) *Proc. Natl. Acad. Sci. U. S. A.* **87**, 6388–6392
- Baldwin, R. L. (1989) *Trends Biochem. Sci.* **14**, 291–294
- Karplus, M., and Weaver, D. L. (1994) *Protein Sci.* **3**, 650–668
- Vrhovski, B., Jensen, S., and Weiss, A. S. (1997) *Eur. J. Biochem.* **250**, 92–98
- Urry, D. W., Peng, S. Q., and Parker, T. M. (1992) *Biopolymers* **32**, 373–379
- Tanford, C. (1973) *The Hydrophobic Effect: Formation of Micelles and Biological Membranes*, pp. 16–24, John Wiley & Sons, Inc., New York
- Lorch, M., Mason, J. M., Clarke, A. R., and Parker, M. J. (1999) *Biochemistry* **38**, 1377–1385